Available online at www.sciencedirect.com

ScienceDirect

Journal of Taibah University for Science 10 (2016) 437–441

Journal of Taibah University for Science

www.elsevier.com/locate/jtusci

Ultra-violet C absorption and LPG sensing study of zinc sulphide nanoparticles deposited by a flame-assisted spray pyrolysis method

K.R. Nemade [a,*], S.A. Waghuley [b]

[a] *Department of Physics, Indira College, Kalamb 445 401, India*
[b] *Department of Physics, Sant Gadge Baba Amravati University, Amravati 444 602, India*

Received 17 April 2015; received in revised form 7 July 2015; accepted 7 July 2015
Available online 31 August 2015

Abstract

Solvent processed spray pyrolysis is a technique that has attracted worldwide interest for the synthesis of nanoparticles. Zinc sulphide (ZnS) belongs to a category of practical semiconductors known as metal sulphides, and it is used extensively as an optical material. In the present article, ZnS nanoparticles were successfully synthesized using flame-assisted spray pyrolysis. X-ray diffraction confirmed the formation of ZnS with an excellent crystalline structure, while scanning electron microscopy indicated that the as-synthesized materials were nanoparticles. Ultraviolet–visible spectroscopy was utilized to evaluate the optical property of the resulting product and revealed that ZnS nanoparticles have the capacity to absorb ultra-violet C. In addition, various liquefied petroleum gas (LPG) sensing properties of the ZnS nanoparticles were also evaluated.

Keywords: Flame assisted; Spray pyrolysis; ZnS nanoparticles; LPG; Ultra-violet C

1. Introduction

Zinc sulphide (ZnS) is one of the most important semiconductor materials and has remarkable properties and holds promise for use in various applications, such as field-emission phenomena, field-effect transistors, luminescence and biosensors [1].

Pathak et al. reported the mechanochemical synthesis of 4–7-nm ZnS nanoparticles with optical band gaps of 4.04–4.6 eV [2]. Dehghani et al. described the nonlinear optical properties of ZnS nanoparticles that were synthesized by a simple chemical method and used PVP (poly vinylpyrrolidone) as a capping agent [3]. Murugadoss et al. successfully synthesized Ni^{2+}-doped ZnS nanoparticles using an aqueous chemical precipitation method with surfactants in air and then studied their photoluminescence properties [4]. Hudlikar et al. demonstrated a green and low-cost synthesis of ZnS nanoparticles using a 0.3% latex solution prepared from *Jatropha curcas* [5].

Xu et al. prepared ZnS nanoparticles by an ultrasonic radiation method and studied their optical properties [6]. Abbas et al. prepared ZnS nanoparticles in an aqueous solution at pH = 3 by a simple reaction between zinc

* Corresponding author. Tel.: +91 9049703051.
E-mail address: krnemade@gmail.com (K.R. Nemade).
Peer review under responsibility of Taibah University.

Production and hosting by Elsevier

http://dx.doi.org/10.1016/j.jtusci.2015.07.003

chloride and sodium sulphide [7]. Yu et al. reported the ethanol sensing abilities of ZnO/ZnS nanocages that were successfully synthesized via a facile hydrothermal route and a subsequent etching treatment [8].

Gas sensing is an important application of metal sulphides, and it is strongly influenced by various parameters such as particle size, particle shape, pore density and surface states. All of these parameters are readily controlled through nanotechnology [9]. Compagnone et al. reported a biological application of gas sensing by demonstrating the detection of food aromas. In this work, gold nanoparticles were used to prepare an array of peptides for the detection of food aromas [10]. The gas sensing process is indirectly related to the band gaps of the used nanomaterials. According to the hyperbolic band model and the effective mass approximation, a particle's size and its band gap are inversely related to each other, which is a widely accepted principle of nanotechnology [11].

From a survey of the materials science literature, it is observed that there are very few examples of ZnS utilized in gas sensing applications. ZnS nanobelts, synthesized using a thermal evaporation method, were used for oxygen sensing by Liu et al. [12]. Yang et al. also reported on an oxygen sensing application of ZnS microspheres that were synthesized by a soft template-assisted hydrothermal route [13].

In the present work, we synthesized ZnS nanoparticles by a flame-assisted spray pyrolysis route. To the best of our knowledge, this study represents a novel approach to ultra-violet C absorption and liquefied petroleum gas (LPG) sensing applications using ZnS nanoparticles.

2. Experimental

Zinc nitrate [$Zn(NO_3)_2$] and sodium sulphide (Na_2S) were of analytical grade (99.99%). The ZnS nanoparticles were prepared by flame-assisted spray pyrolysis. For this synthesis, stock solutions of 1 M $Zn(NO_3)_2$ and 1 M Na_2S were prepared by dissolving a suitable quantity of solute in deionized water having a resistivity close to 18 MΩ cm. The prepared solutions were subjected to rapid magnetic stirring for 30 min at room temperature. Subsequent to this step, the prepared solutions were mixed together in drop-wise manner and then loaded into the chamber for spray pyrolysis. A capillary tube with an outer diameter of 1 mm (inner diameter 0.6 mm) and an opening of 1.2 mm in diameter (Labtronics, India) was employed. The spray was evaporated by supporting flamelets maintained at 473 K, and the flow rate was regulated by a flow controller. The product was collected on a SiO_2 substrate.

The as-prepared ZnS nanoparticles were characterized by X-ray diffraction (XRD), scanning electron microscopy (SEM) and ultraviolet–visible (UV–VIS) spectroscopy. The XRD pattern was obtained from a Rigaku Miniflex-II diffractometer over a range of 10–70°. The morphology and grain size of the sample were studied by using SEM (JEOL JSM-7500F). UV–VIS spectroscopy was performed on a Perkin Elmer UV spectrophotometer.

The ZnS nanoparticles deposited on a SiO_2 substrate were used as a chemiresistive film [14]. For sensing measurements, electrodes of highly conducting silver were created by applying silver paint to adjacent sides of the

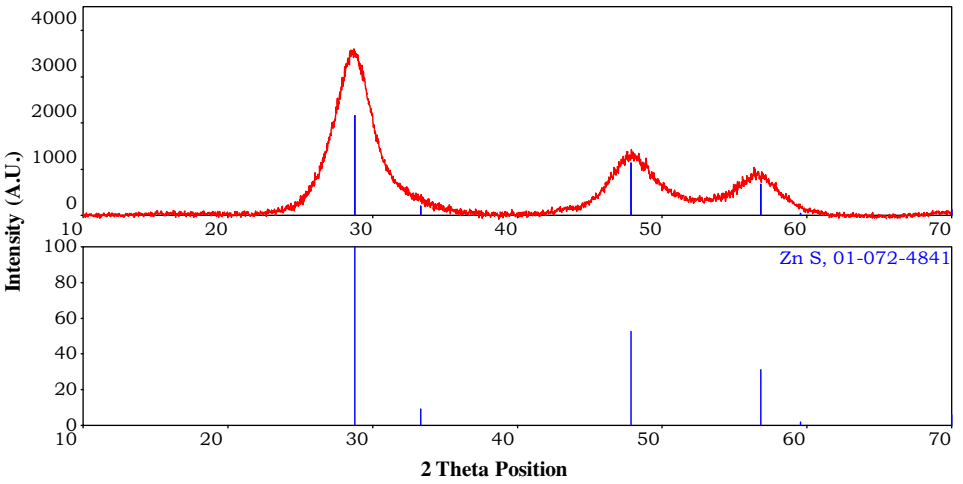

Fig. 1. XRD pattern of as-synthesized ZnS nanoparticles.

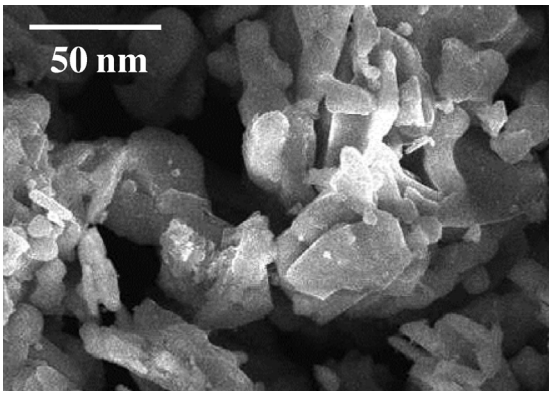

Fig. 2. SEM image of ZnS nanoparticles.

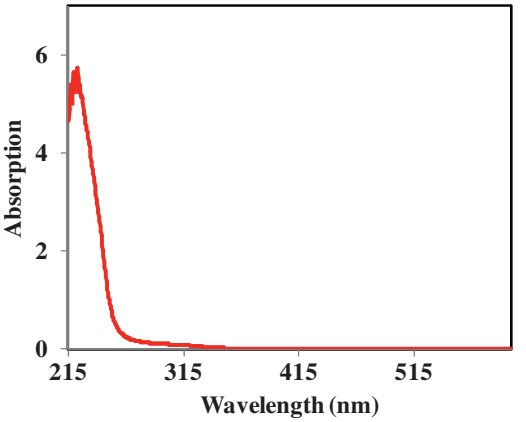

Fig. 3. UV–VIS spectra of as-synthesized ZnS nanoparticles.

film and then heating at 80 °C for 25 min. The change in electrical resistance was determined by the voltage drop method [15]. The sensing response was defined as in [16]. The required gas concentration inside the system was achieved by the injection syringe method [17].

3. Results and discussion

Fig. 1 shows the XRD pattern of as-synthesized ZnS nanoparticles. The pattern contains three main diffraction peaks indexed as (1 1 1), (2 2 0), and (3 1 1) and are well matched with the standard card for cubic ZnS (JCPDS no. 01-072-4841). The characteristic peaks in the pattern are broadened due to the small size of the particles, which clearly indicates the presence of nanoparticles. The size of the as-synthesized nanocrystals was determined by Scherrer's equation [18] and was found to be 7.9 nm.

The particle size and morphology of as-prepared nanocrystalline ZnS were evaluated. A typical SEM micrograph of ZnS nanoparticles is shown in Fig. 2. The image clearly reveals that the synthesized ZnS has a particle size on the order of ∼8 nm. Furthermore, the micrograph shows the presence of aggregated nanoparticles.

The UV–VIS absorption spectrum of as-synthesized ZnS nanoparticles in an aqueous medium was recorded from 215 to 600 nm, as shown in Fig. 3; before the start of the measurement, deionized water was used for a baseline correction. An absorption peak was observed near 221 nm, which indicates the presence of the quantum confinement effect in ZnS nanoparticles [19]. The optical band gap of the nanocrystals was determined using the energy wave equation ($E = hc/\lambda$), which was found to be 5.6101 eV. This study shows that as-synthesized ZnS nanoparticles absorb in the region between 200 and 250 nm, which suggests that this material may be used as ultraviolet-blocking materials, especially for ultra-violet C radiation.

Fig. 4(a) shows the LPG sensing response of ZnS nanoparticles at room temperature. The response curve is nearly linear up to 400 ppm, which shows that the saturation limit for ZnS nanoparticles is beyond 400 ppm.

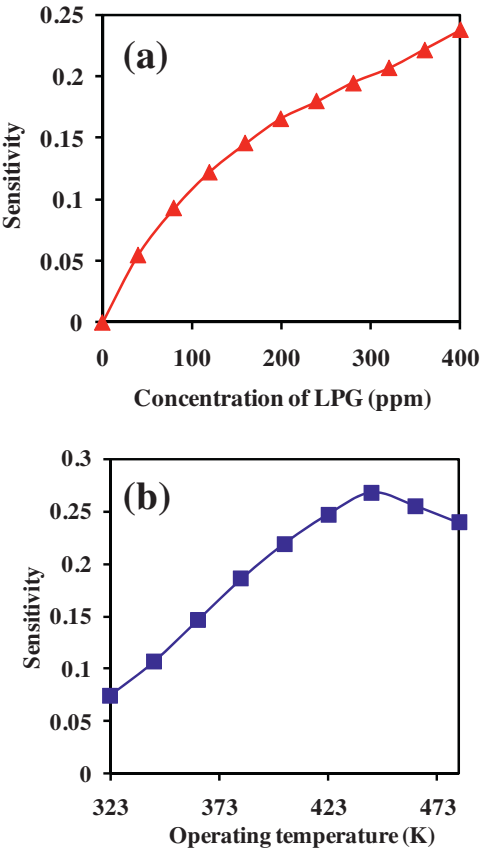

Fig. 4. LPG sensing response (a) at room temperature and (b) the operating temperature response for 200 ppm LPG.

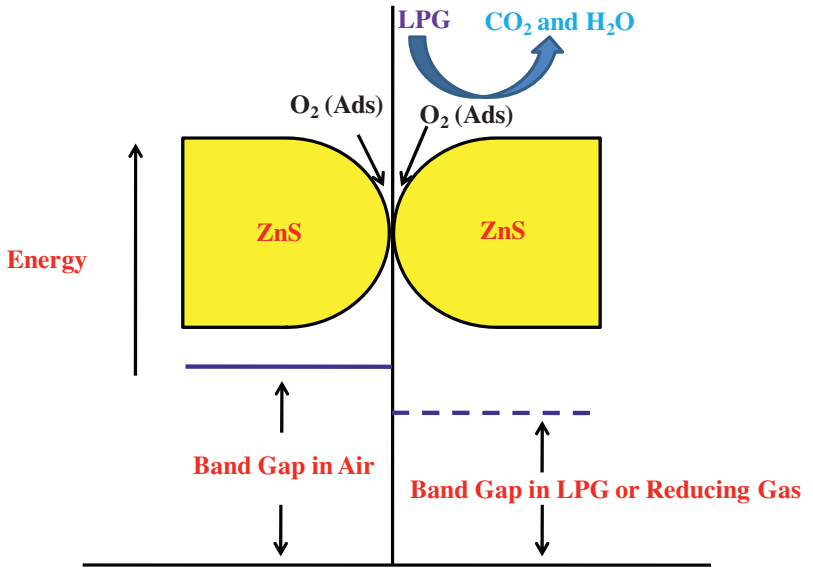

Fig. 5. Plausible LPG sensing mechanism.

This also reveals that the change in resistance of the as-synthesized sensing material displays a good dependence on the LPG concentration. In the presence of LPG (reducing species), the resistance of the ZnS nanoparticles decrease, which suggests that ZnS nanoparticles are intrinsically n-type. Fig. 4(b) presents the operating temperature response of a ZnS sensing film for 200 ppm LPG. From the plot, it is clearly observed that the sensing response increases at 443 K. Beyond this temperature the response begins to decrease. This may be due to the desorption of atmospheric oxygen species. As the temperature increases, the thermal energy of the sensing surface increases, and this promotes desorption [20].

A plausible explanation for the LPG-sensing mechanism is illustrated in Fig. 5. It is well known that atmospheric oxygen adsorbs on sensing materials, from which the oxygen acquires conduction band electrons. It is also well known that LPG is a mixture of reduction agents such as CH_4, C_3H_8 and C_4H_{10}. As the LPG interacts with the sensing surface and adsorbed oxygen, H_2O and CO_2 are formed as sensing side products (Eqs. (1) and (2)) [21].

$$C_nH_{2n+2} + 2O^-(\text{ads}) \rightarrow H_2O + C_nH_{2n}{:}\,O + e^- \quad (1)$$

$$C_nH_{2n}{:}\,O + O^-(\text{ads}) \rightarrow CO_2 + H_2O + e^- \quad (2)$$

Fig. 6 depicts the response stability of ZnS nanoparticles measuring 200 ppm LPG at room temperature. Responses were recorded for a total of 30 days at 5-day intervals. This plot reflects the good stability of ZnS nanoparticles against LPG. The inset of Fig. 6 shows the transient response of ZnS nanoparticles indicating that the ZnS based sensor has response time on the order of 18 s and fast recovery of 11 s.

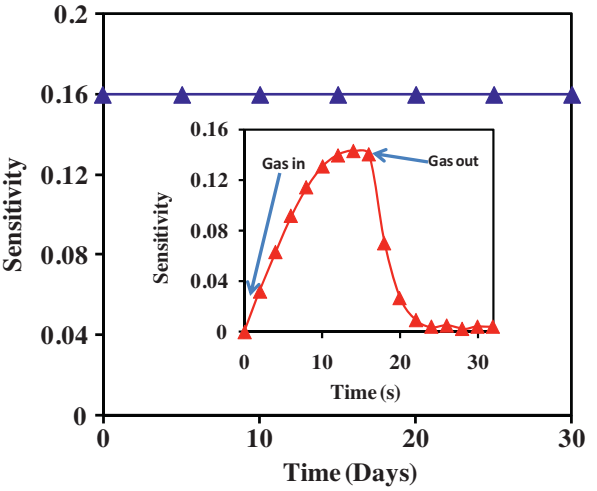

Fig. 6. Stability response of ZnS nanoparticles against LPG. The inset shows the transient response at room temperature.

4. Conclusions

In this paper, we reported a flame-assisted spray pyrolysis synthesis of ZnS nanoparticles. The XRD pattern and SEM image indicate the formation of ZnS nanoparticles approximately 8 nm in size. UV–VIS absorption spectra showed a strong absorption peak

near 221 nm, which suggests that the ZnS nanoparticles may be employed as a practical ultra-violet C absorber. In addition, the as-synthesized ZnS nanoparticles were successfully employed for LPG sensing. Different sensing parameters such as sensing response at room temperature, operating temperature, transient response and stability were evaluated and explained. The linear response to the analyte, the operating temperature and the fast transient response reveal that the ZnS sensor reported in this work satisfies the requirements of a practical sensor.

Acknowledgments

The authors are wish to thank the head of the Department of Physics, Sant Gadge Baba Amravati University, Amravati for the use of their facilities. One of the authors, Kailash Nemade, is very grateful to the principal of Indira College, Kalamb, for providing academic assistance.

References

[1] X. Fang, T. Zhai, U.K. Gautam, L. Li, L. Wu, Y. Bando, D. Golberg, ZnS nanostructures: from synthesis to applications, Prog. Mater. Sci. 56 (2011) 175–287.

[2] C.S. Pathak, M.K. Mandal, V. Agarwala, Synthesis and characterization of zinc sulphide nanoparticles prepared by mechanochemical route, Superlattices Microstruct. 58 (2013) 135–143.

[3] Z. Dehghani, S. Nazerdeylami, E. Saievar-Iranizad, M.H. Majles Ara, Synthesis and investigation of nonlinear optical properties of semiconductor ZnS nanoparticles, J. Phys. Chem. Solids 72 (2011) 1008–1010.

[4] G. Murugadoss, M. Rajesh Kumar, Synthesis and optical properties of monodispersed Ni^{2+}-doped ZnS nanoparticles, Appl. Nanosci. 4 (2014) 67–75.

[5] M. Hudlikar, S. Joglekar, M. Dhaygude, K. Kodam, Latex-mediated synthesis of ZnS nanoparticles: green synthesis approach, J. Nanopart. Res. 14 (2012) 865–871.

[6] J.F. Xu, W. Ji, J.Y. Lin, S.H. Tang, Y.W. Du, Preparation of ZnS nanoparticles by ultrasonic radiation method, Appl. Phys. A 66 (1998) 639–641.

[7] N.K. Abbas, K.T. Al-Rasoul, Z.J. Shanan, New method of preparation ZnS nano size at low pH, Int. J. Electrochem. Sci. 8 (2013) 3049–3056.

[8] X. Yu, H. Ji, H. Wang, J. Sun, X. Du, Synthesis and sensing properties of ZnO/ZnS nanocages, Nanoscale Res. Lett. 5 (2010) 644–648.

[9] T. Kida, S. Fujiyama, K. Suematsu, M. Yuasa, K. Shimanoe, Pore and particle size control of gas sensing films using SnO_2 nanoparticles synthesized by seed-mediated growth: design of highly sensitive gas sensors, J. Phys. Chem. C 117 (2013) 17574–17582.

[10] D. Compagnone, G.C. Fusella, M. Del Carlo, P. Pittia, E. Martinelli, L. Tortora, R. Paolesse, C. Di Natale, Gold nanoparticles-peptide based gas sensor arrays for the detection of food aromas, Biosens. Bioelectron. 42 (2013) 618–625.

[11] K.R. Nemade, S.A. Waghuley, Synthesis and characterization of bismuth oxide quantum dots, Adv. Sci. Eng. Med. 5 (2013) 988–990.

[12] Y.G. Liu, P. Feng, X.Y. Xue, S.L. Shi, X.Q. Fu, C. Wang, Y.G. Wang, T.H. Wang, Room-temperature oxygen sensitivity of ZnS nanobelts, Appl. Phys. Lett. 90 (2007) 042109–042112.

[13] L. Yang, J. Han, T. Luo, M. Li, J. Huang, F. Meng, et al., Morphogenesis and crystallization of ZnS microspheres by a soft template-assisted hydrothermal route: synthesis, growth mechanism, and oxygen sensitivity, Chem. Asian J. 4 (2009) 174–180.

[14] K.R. Nemade, S.A. Waghuley, Optical and gas sensing properties of CuO nanoparticles grown by spray pyrolysis of cupric nitrate solution, Int. J. Mater. Sci. Eng. 1 (2014) 63–66.

[15] K.R. Nemade, S.A. Waghuley, Strontium oxide quantum dot decorated graphene composites for liquid petroleum gas sensing, J. Chin. Adv. Mater. Soc. 1 (2013) 219–228.

[16] K.R. Nemade, S.A. Waghuley, Role of defects concentration on optical and carbon dioxide gas sensing properties of Sb_2O_3/graphene composites, Opt. Mater. 36 (2014) 712–716.

[17] K.R. Nemade, S.A. Waghuley, LPG sensing application of graphene/Bi_2O_3 quantum dots composites, Solid State Sci. 22 (2013) 27–32.

[18] K.R. Nemade, S.A. Waghuley, LPG sensing application of graphene/CeO_2 quantum dots composite, AIP Conf. Ser. 1536 (2013) 1258–1259.

[19] K.R. Nemade, S.A. Waghuley, Low temperature synthesis of semiconducting α-Al_2O_3 quantum dots, Ceram. Int. 40 (2014) 6109–6113.

[20] K.R. Nemade, S.A. Waghuley, Chemiresistive gas sensing by few-layered graphene, J. Electron. Mater. 42 (2013) 2857–2866.

[21] K.R. Nemade, S.A. Waghuley, Preparation of MnO_2 immobilized graphene nanocomposite by solid state diffusion route for LPG sensing, J. Lumin. 153 (2014) 194–197.